Environmental Science: Atmospheres

ROYAL SOCIETY OF CHEMISTRY

PAPER

View Article Online
View Journal | View Issue

Cite this: *Environ. Sci.: Atmos.*, 2023, **3**, 1296

Theoretical study on the aqueous phase oxidation of glyoxal†

Bo Wei, [abcd] Ruifeng Zhang,[abc] Patrick H.-L. Sit, [*ab] Maoxia He[d] and Chak K. Chan ‡[*abe]

Received 31st March 2023
Accepted 20th July 2023

DOI: 10.1039/d3ea00049d

rsc.li/esatmospheres

Glyoxal (GLY) is an important precursor of aqueous secondary organic aerosol (aqSOA). Knowledge of the reaction mechanisms of GLY in the aqueous phase is not complete, and the oxidation mechanisms of GLY in the presence of different oxidants are under debate. Our recent experimental studies of GLY oxidation mediated by nitrate photolysis yielded formic acid instead of oxalic acid which was commonly found in bulk GLY oxidation experiments. In this work, we investigated the hydration and oligomer formation mechanism of GLY in the aqueous phase theoretically. Furthermore, we calculated the energetics for the mechanisms of GLY oxidation by OH radicals in the presence of O_2 and NO_2. Results showed that the hydration reaction plays a significant role in GLY uptake into the aqueous phase, and oligomers are likely to form at intermediate RH. The formation of formic acid in the presence of OH and NO_2 is more favorable, while oxalic acid is the main product in the presence of OH and O_2. The present study provides a theoretical insight into the aqueous-phase chemistry of GLY, and the results may be helpful for understanding the atmospheric evolution of GLY.

Environmental significance

Glyoxal (GLY) is an important precursor of aqueous secondary organic aerosol (aqSOA). We have previously reported formic acid/formate production as the main oxidation product from the photooxidation of glyoxal during particulate sodium nitrate photolysis (*Environ. Sci. Technol.*, 2021, **55**, 9, 5711–5720). To better understand these reactions, we calculated the energetics for the mechanisms of glyoxal oxidation by OH radicals in the presence of O_2 and NO_2. Results showed that the formation of formic acid in the presence of OH and NO_2 is more favorable, while oxalic acid is the main product in the presence of OH and O_2. Furthermore, the hydration reaction plays a significant role in glyoxal uptake into bulk solutions or cloud droplets, and oligomers are likely to form at intermediate relative humidity. Our study provides a theoretical insight into the aqueous-phase chemistry of glyoxal, and the results may be helpful for understanding the atmospheric evolution of glyoxal under different oxidative environments.

1. Introduction

Glyoxal (GLY) is the simplest α-dicarbonyl intermediate product from the atmospheric oxidation of biogenic VOCs such as isoprene[1–3] and anthropogenic precursors such as isoprene and aromatics,[4,5] primarily emitted from biomass burning and vehicle emission, respectively.[5,6] Glyoxal can exist in the gas phase, the air–water interface, and the aqueous phase. The major removal processes of glyoxal have been reported to be gas-phase photolysis,[7,8] with a lifetime $\Gamma_{photo} \approx 2$ to 3 h. Due to its atmospheric abundance and high effective Henry's law constant, aqueous chemistry of glyoxal has been shown as an important source of SOA *via* cloud processing.[9–13] In addition, Zhang *et al.*[14] reported that glyoxal interfacial photochemistry may elevate its uptake onto the aqueous surface, contributing to aqSOA formation, surface activity, and aerosol nucleation as a result of multiphase chemistry.

GLY in cloud/fog droplets and aerosol particles undergoes a series of atmospheric processes such as photolysis, photochemical oxidation, acid/ammonium-catalyzed reactions, and oligomerization to form carboxylic acid, oligomers, organosulfate, and nitrogen-containing organics as SOA.[10,15] Several experimental and theoretical studies have examined the photooxidation of GLY.[16–19] Aqueous-phase OH oxidation of GLY can generate low volatile products contributing to the formation of SOA in the atmosphere.[20,21] Furthermore, brown carbon (BrC), a significant factor in assessing aerosol radiative climate

[a]*School of Energy and Environment, City University of Hong Kong, Tat Chee Avenue, Kowloon, Hong Kong 999077, China. E-mail: patrick.h.sit@cityu.edu.hk; chak.chan@kaust.edu.sa; chak.k.chan@cityu.edu.hk*

[b]*City University of Hong Kong Shen Zhen Research Institute, Shen Zhen 518057, China*

[c]*College of Safety and Environmental Engineering, Shandong University of Science and Technology, Qingdao, 266590, China*

[d]*Environment Research Institute, Shandong University, Qingdao, 266237, China*

[e]*Low-Carbon and Climate Impact Research Centre, City University of Hong Kong, Hong Kong 999077, China*

† Electronic supplementary information (ESI) available. See DOI: https://doi.org/10.1039/d3ea00049d

‡ Current Address: Division of Physical Science and Engineering, King Abdullah University of Science and Technology, Thuwal, 23955-6900, Saudi Arabia.

effects,[22] can be formed when GLY reacts with ammonia in ammonium containing solutions.[23,24]

Knowledge of the reaction mechanisms of GLY in the aqueous phase is not complete, and the oxidation mechanisms of GLY in the presence of different oxidants are under debate. Using H_2O_2 photolysis as the source of OH radicals, low-volatility compounds such as glyoxylic acid and oxalic acid[10,20,25] have generally been reported while formic acid, a volatile species, was found in some studies.[21,25] Recently, we reported that formic acid/formate was the main oxidation product of glyoxal during particulate sodium nitrate photolysis.[26] Nitrate photolysis can produce a series of reactive species, including OH radicals, NO_2, and N(III) (NO_2^-/HONO).[27,28] Whether the presence of reactive nitrogen species (*e.g.*, NO_2) modifies the mechanism of GLY oxidation and promotes the formation of formic acid/formate deserves further investigation.

In this study, we first investigated the hydration and oligomer formation mechanism of GLY in aqueous phase theoretically. We calculated the energetics for the mechanisms of GLY oxidation by OH radicals in the presence of O_2 and NO_2. The oxidation mechanisms of GLY under other oxidative environments (O_3, HO_2 and H_2O_2) were also determined. We found that the hydration reaction plays a significant role in GLY uptake into diluted bulk solutions and cloud/fog droplets, and oligomers are likely to form at intermediate relative humidity. Furthermore, the formation of formic acid in the presence of OH and NO_2 is more favorable, while oxalic acid is the main product in the presence of OH and O_2. Overall, in the aqueous phase, reaction with OH radicals is the primary initial loss process for glyoxal, compared to reactions with O_3, HO_2, and H_2O_2. Our study provides a theoretical insight into the aqueous-phase chemistry of GLY, and the results may be helpful for understanding the atmospheric evolution of GLY.

2. Computational methods

All of the electronic structure calculations were conducted using the Gaussian 16 program[29] employing the M06-2X[30] method with the 6-31+G(d,p) basis set. The M06-2X functional has been shown to be reliable to predict the geometries and frequencies of the stationary points[31,32] and thermodynamic data for main-group elements.[33,34] We also calculated the energy barrier of gas phase reaction GLY·$2H_2O$ to IM5 by using CCSD(T) with the aug-cc-pvTz basis set at the optimized geometry to verify the reliability of results. As shown in Table S5,† the energy barrier calculated by M06-2X/6-311++G(3df,2p)//M06-2X/6-31+G(d,p) was 7.04 kcal mol^{-1}, while the energy barrier calculated by CCSD(T)/aug-cc-pvTz//M06-2X/6-31+G(d,p) was 7.77 kcal mol^{-1}. Considering the computational cost and accuracy, the methods used in this work are reliable. The vibrational frequencies at the same level were used to verify all stationary points as either the transition state (TS, only one imaginary frequency) or the minima (zero imaginary frequency). The reaction pathways were confirmed by intrinsic reaction coordinate (IRC) analysis. The single point energies of the optimized structures were further calculated with the 6-311++G(3df,2p) basis set, and the thermal corrections and the basis set superposition error (BSSE) corrections were also included in the potential energies. The continuum solvation model 'SMD' was used to determine the solvent effect of water.[35] The reaction kinetics was calculated with transition-state theory (TST) based on the KiSThelP[36] program. Because of the interaction between GLY, GLY·$1H_2O$, and water molecules, the geometries of GLY and GLY·$1H_2O$ with water complex were also determined. Such interaction was also considered for the energy barriers calculation of hydration processes. The complexes of GLY with oxidants were not investigated in the oxidation pathways, due to the minor impact of molecular interaction.

The trans form of glyoxal was used in this study, because it is more easily solvated in the bulk.[37] We optimized the conformers of transition state for the GLY·$1H_2O$ to IM2 reaction (Fig. 2). The structures of the conformers are shown in Table S3.† We calculated the energy barriers for the conformers in the gas phase and aqueous phase. As shown in Table S4,† the solvation effects cause a significant change in the energy barriers of the transition state conformers. The solvent changes the order of these relative energy values, from $a < d < c < b$ in the gas phase to $a < d < b < c$ in the aqueous phase. Further studies are needed to confirm the solvation effect on the relative energies of conformers. However, regardless of these solvation effects, the trend of the reactivity of different oxidants toward GLY remains valid, because the difference between the relative energies of the transition state conformers in any of the oxidation reaction is less than 2 kcal mol^{-1}.

The atmospheric lifetime can be estimated as:

$$\tau = \frac{1}{k[\text{oxidant}]}$$

where k represents the rate constant of the reactant with the oxidant and [oxidant] represents the atmospheric concentration of the oxidant.

3. Results and discussion

3.1 Glyoxal hydration and oligomer mechanism

Before we present the results of oxidation of GLY, it is useful to discuss its hydration characteristics. The hydration of GLY to produce glyoxal–diol (GLY·$1H_2O$) is an important initiation reaction for GLY in the aqueous formation of SOA and BrC in the atmosphere.[38,39] Once formed, the glyoxal–diol (GLY·$1H_2O$) can undergo further hydrolysis to form the glyoxal dihydrate (GLY·$2H_2O$) (Fig. 1). Furthermore, two glyoxal–diols can combine to form the open dimer IM1. Intramolecular nucleophilic attack on the sp^2 carbon of IM1 can yield two possible ring structures: the five-membered dioxolane ring dimer P1 and the six-membered dioxane ring dimer P2. Formation of both rings from IM1 is thermodynamically favorable but the ring closure to form P1 has a relatively lower barrier ($\Delta G^{\ddagger}$ = 14.34 kcal mol^{-1}) than P2 ($\Delta G^{\ddagger}$ = 18.36 kcal mol^{-1}). The formation of P1 is also thermodynamically more favorable (ΔG = −12.36 kcal mol^{-1}) than P2 (ΔG = −5.89 kcal mol^{-1}). Hence, P1 is more likely to be formed, in agreement with experimental results.[40–42]

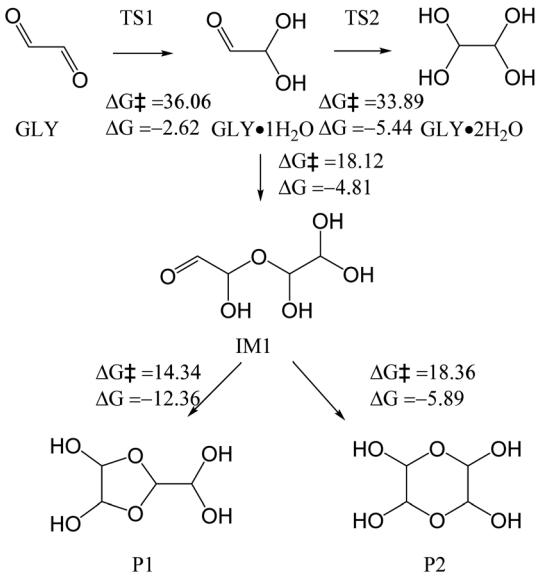

Fig. 1 The hydration and polymerization mechanism of glyoxal.

The formation of GLY·2H_2O is a two-step hydrolysis reaction. The energy barriers for the above hydrolysis reactions (*via* TS1 and TS2) with the addition of one water molecule are high, at 36.06 and 33.89 kcal mol^{-1}, respectively. We investigated the hydrolysis reactions by introducing extra water molecules to participate in the hydrolysis reactions in the implicit solvent model. The geometries of GLY and GLY·1H_2O with water complex were determined, as depicted in Fig. S1-1 and S1-2.† The structures of TS1 and TS2 with extra water molecules are summarized in Fig. S2 and S3.† The hydrogen atom from water molecules can attach to the aldehyde group of GLY, while the hydroxyl group (–OH) can attach to the carbon atom of GLY. When the extra water molecules are involved, they act as a bridge to the aldehyde, thus making the hydration reaction more likely to occur. As illustrated in Table S1,† when there are four water molecules in the reactions, the barriers decrease to 11.64 and 14.57 kcal mol^{-1} for TS1 and TS2, respectively. Water molecules have a catalytic effect in lowering the energy barriers for the hydrolysis reaction. Hence when the humidity increases, it is possible for more water molecules to participate and facilitate the hydration reactions and GLY is likely in the GLY·2H_2O form. In addition, Rypkema *et al.*[43] and Long *et al.*[31] reported that carboxylic acids and sulfuric acid can act effectively as catalysts in the hydration of aldehydes. Hence, the uptake of glyoxal can be facilitated in complex atmospheric aqueous aerosol.[19,44] In cloud droplets, with the concentrations in the range of μM, GLY predominantly exists in GLY·2H_2O form.[45] In aerosol droplets, GLY·1H_2O may also be important.

3.2 Aqueous oxidation pathways of GLY to form low volatility organic acids

Previous studies focused on the aqueous oxidation of GLY by OH radicals generated from the H_2O_2 photolysis.[10,21,25] In such situations, the OH radicals and H_2O_2 are the main oxidants, and they promote the formation of low-volatility organic acids (*e.g.*, oxalic acid and glyoxylic acid). These first-generation oxidants can also undergo further radical chain reactions to form second-/third-generation oxidants (*e.g.*, O_3 and HO_2). Hence, we investigated the reaction mechanisms of GLY and these oxidants using quantum chemistry calculation.

3.2.1 The oxidation of GLY by OH radical. As mentioned above, GLY predominantly (98%) exists in GLY·2H_2O form in bulk solutions and cloud/fog droplets.[19,46] As shown in Fig. 2, GLY·2H_2O can react with OH radicals to generate IM5 that transforms to IM7 *via* subsequent molecular oxygen addition and HO_2 radical elimination. IM7 can react with OH radical to form the glyoxylic acid alkyl radical IM8, which undergoes oxygen addition reaction and HO_2 elimination to finally yield oxalic acid P3. The energy barriers through this pathway are generally low, 7.31–8.69 kcal mol^{-1}, which means that oxalic acid is likely to form in the presence of oxygen. The mechanism is consistent with the radical reactions proposed in previous studies.[19,25] We also investigated the mechanism of GLY·1H_2O. OH radical reacts with GLY·1H_2O *via* H atom abstraction to form the glyoxal radical IM2, which can further react with molecular oxygen to form the glyoxal peroxyl radical IM3, which forms glyoxylic acid IM4 after an HO_2 radical elimination. This

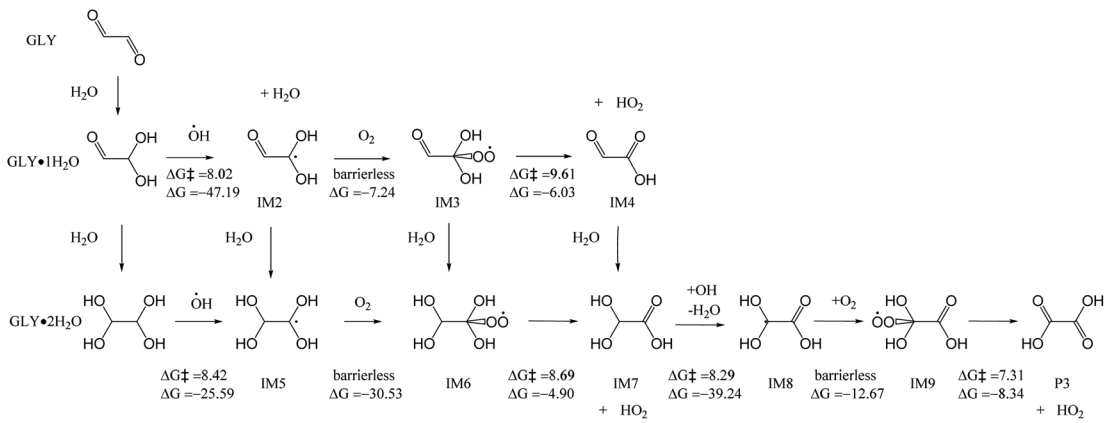

Fig. 2 Mechanisms for the reactions of GLY with OH radicals and O_2 in the aqueous phase, with the energy barrier ($\Delta G^{\ddagger}$) and reaction energy (ΔG) (kcal mol^{-1}).

mechanism can explain experimental observations of glyoxylic acid and oxalic acid in aqueous reactions of GLY in H_2O_2 photolysis.[10,21,25]

Furthermore, two IM6 molecules can yield IM10 by RO_2–RO_2 reaction[10,47] (Fig. 3a). IM10 undergoes subsequent decomposition to yield IM11, IM12, and IM13. IM12 can also react with O_2 to form the peroxyl radical IM14, which undergoes a HO_2 elimination to generate formic acid P4. However, due to the high energy barrier between IM10 and IM12 (35.55 kcal mol^{-1}), this reaction is not expected to occur easily. Fig. 3b shows that IM6 can also react with NO to form intermediate IM15, followed by the NHO_2 elimination to form IM16. IM16 finally decomposes to formic acid, CO_2 and H_2O. However, the energy barrier between IM15 and IM16 is 26.68 kcal mol^{-1}, which is quite high and hinders the reaction. The above two pathways of IM6 can end up in formic acid, however, they both have a step with a relative high energy barrier. Hence, they may not be the main pathway to form formic acid.

Alternatively, the formed glyoxal peroxyl radical IM3 (Fig. 2), an RO_2, can also undergo a RO_2–RO_2 reaction to form IM17 (Fig. 3c). IM17 decomposes to carbon monoxide, IM13, and IM18, with the energy barrier of 51.25 kcal mol^{-1}. IM13 transforms into water and carbon dioxide, while IM18 transforms into water and IM4. IM4 likely undergoes hydration reaction to form IM7 (Fig. 2) and oxalic acid P3 eventually. Because of the high energy barrier (51.25 kcal mol^{-1}), the above RO_2–RO_2 pathway is not feasible energetically. IM3 can also react with NO, followed by the NHO_2 elimination, finally decomposes to formic acid and CO_2, which is also not likely to occur, due to the high energy barrier (40.90 kcal mol^{-1}) (Fig. 3d). Overall, OH reactions with GLY can form glyoxylic acid and oxalic acid, but not likely formic acid.

3.2.2 The oxidation of GLY by H_2O_2. Recent studies have reported hydroxyhydroperoxide (HHP) formation from reactions between H_2O_2 and GLY.[48–50] HHP is formed *via* the nucleophilic attack of an O atom from H_2O_2 to the carbonyl

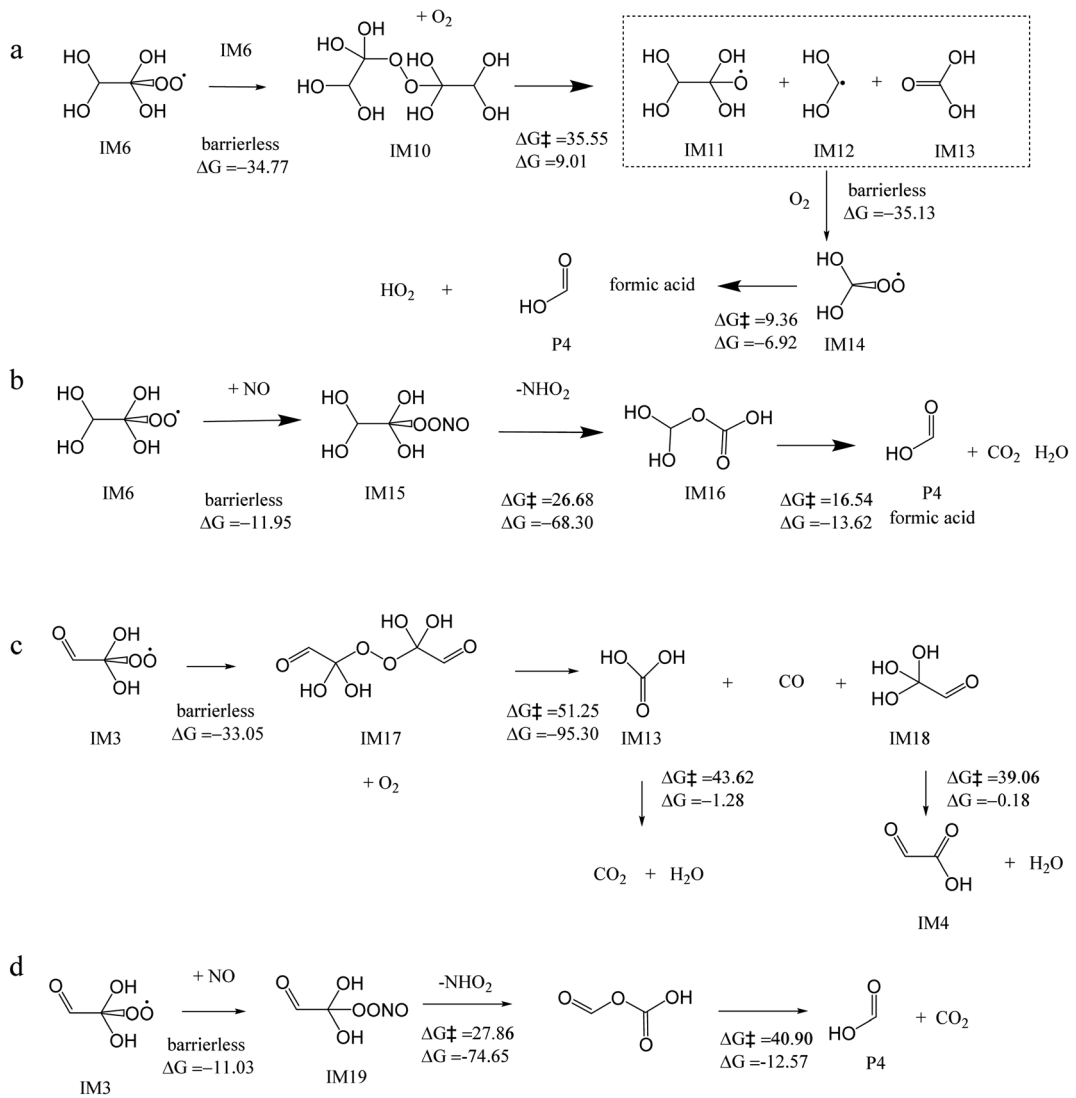

Fig. 3 Mechanisms for the subsequent reactions of IM3 and IM6 in the aqueous phase, with the energy barrier ($\Delta G^{\ddagger}$) and reaction energy (ΔG) (kcal mol^{-1}), to produce formic acid.

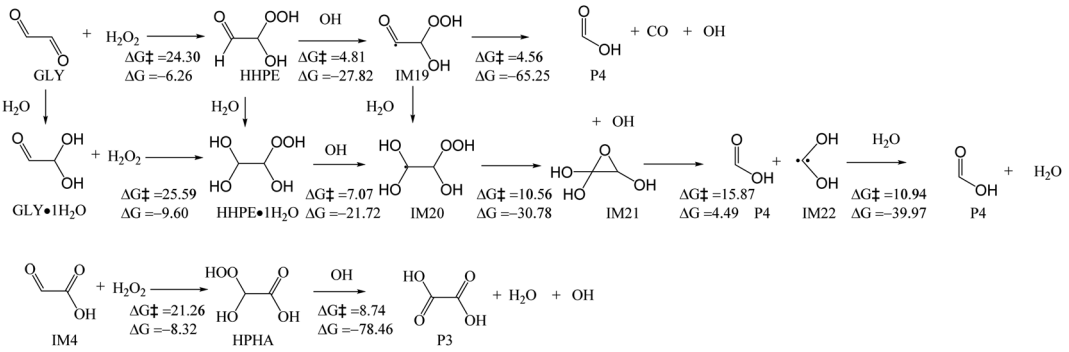

Fig. 4 Mechanisms for the reactions of GLY with H_2O_2 and OH in the aqueous phase, with the energy barrier ($\Delta G^{\ddagger}$) and reaction energy (ΔG) (kcal mol^{-1}).

group, followed by the migration of one of the H atoms of H_2O_2 to the oxygen of the carbonyl group.[51,52] We also calculated the energy barrier of the reaction of GLY and H_2O_2 in the presence of a H_2O molecule. Fig. 4 shows that H_2O_2 reacts with GLY and GLY·$1H_2O$ to form 2-hydroxy-2-hydroperoxyethanal (HHPE) and its hydrated counterpart (HHPE·$1H_2O$), with the energy barriers of 24.30 and 25.59 kcal mol^{-1}, respectively. HHPE can react with OH radical to form acyl radical IM19 by H abstraction, and then IM19 decomposes to formic acid (P4), CO, and OH radical. HHPE·$1H_2O$ can also react with OH to form IM20, and with the elimination of an OH radical to form expoxy intermediate IM21. Through a decomposition reaction, IM21 can transform into formic acid (P4) and IM22. In the presence of water, IM22 can transform to formic acid (P4) by H shift reaction, with the energy barrier of 10.94 kcal mol^{-1}. The glyoxylic acid IM4 can also react with H_2O_2 to form 2-hydroperoxy-2-hydroxyacetic acid (HPHA), with the energy barrier of 21.26 kcal mol^{-1}. Similarly, an OH radical abstracts a H atom from HPHA to form oxalic acid P3, OH and H_2O. The rate constants of reaction GLY and GLY·$1H_2O$ towards H_2O_2 are 2.11 $\times$ 10^{-2} and 1.39 s^{-1} M^{-1}, respectively (Table S2†). The rate constant of reaction IM4 towards H_2O_2 is 6.74 $\times$ 10^{-2} s^{-1} M^{-1}. These rate constants are much lower than those of GLY·$1H_2O$ and GLY·$2H_2O$ reacting with OH (1.52 $\times$ 10^7 and 6.75 $\times$ 10^6 s^{-1} M^{-1}). In our recent study of nitrate photolysis that produces OH radicals in the particles,[26] the model predicted steady-state concentration of H_2O_2 and OH were ~10^{-4} M and ~10^{-15} M, respectively. Using these concentrations as references, the atmospheric aqueous-phase lifetimes (τ) for the initial reaction of GLY and GLY·$1H_2O$ with H_2O_2 were 5.49 days and 0.08 days. The atmospheric aqueous-phase lifetimes (τ) for the initial reaction of GLY·$1H_2O$ and GLY·$2H_2O$ with OH radicals were 761.45 days and 1714.68 days. Although the reactions with H_2O_2 can be competitive to that with OH radicals, the reactions with H_2O_2 are also not dominant pathways to form formic acid, since GLY predominantly exists in GLY·$2H_2O$.

3.2.3 The oxidation of GLY by O_3 and HO_2. Ozone abstracts the most weakly bound H atom of GLY·$1H_2O$ to form OH radical, molecular oxygen, and alkyl radical IM2 [53] (Fig. 5). It has a high energy barrier of 33.03 kcal mol^{-1}. Subsequent reaction with O_2 forms peroxyl radical IM3 which quickly decomposes to form IM4 and HO_2 radical. Similar to GLY·$1H_2O$, GLY·$2H_2O$ can also react with O_3, with the loss of OH and O_2, to form IM5. IM5 transforms to IM6, with the addition of molecular oxygen,

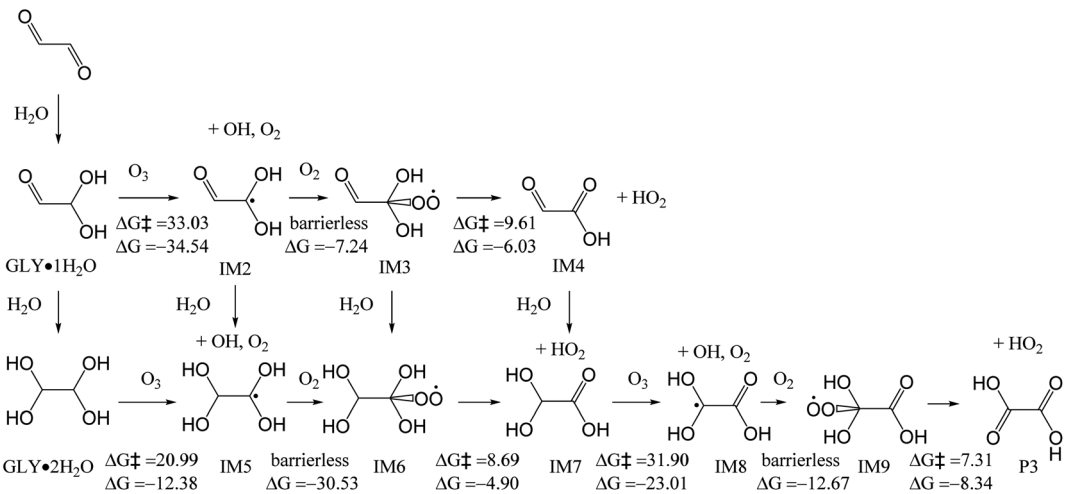

Fig. 5 Mechanisms for the reactions of GLY with ozone and O_2 in the aqueous phase, with the energy barrier ($\Delta G^{\ddagger}$) and reaction energy (ΔG) (kcal mol^{-1}).

followed by HO_2 elimination, to form IM7. The energy barrier between GLY·2H_2O and IM5 is 20.99 kcal mol^{-1}. Similarly, IM7 can also react with O_3, and finally transforms to oxalic acid P3 after a series of reactions. The energy barrier between IM7 and IM8 is 31.90 kcal mol^{-1}. These reactions can therefore be regarded as an additional reaction pathway to form oxalic acid. In reaction with O_3, IM6 is also formed. Hence, it is also possible to form formic acid through RO_2–RO_2 reaction (Fig. 3a) or reaction with NO (Fig. 3b). Considering the high energy barrier of 20.99–33.03 kcal mol^{-1} in the reactions with O_3, these reactions are not as competitive as those with OH radicals as described in last section.

The hydroperoxyl radical (HO_2) is a product of OH-initiated VOC oxidation and carbonyl photolysis,[54] and it can initiate the oxidation of GLY.[55] As depicted in Fig. S4,† HO_2 abstracts an H atom from GLY·1H_2O to form IM2 and H_2O_2, with the energy barrier of 17.82 kcal mol^{-1}. Similarly, GLY·2H_2O reacts with HO_2, with the loss of H_2O_2 to form IM5, with an energy barrier of 19.86 kcal mol^{-1}. IM7 reacts with HO_2, and finally transforms to oxalic acid P3. The energy barrier between IM7 and IM8 is 20.66 kcal mol^{-1}. As shown in Table S2,† the rate constants of reaction GLY·1H_2O and GLY·2H_2O with OH radicals are 10^6 to 10^7 s^{-1} M^{-1} and those of reaction GLY·1H_2O and GLY·2H_2O towards O_3 are 1.90×10^{-10} and 0.14 s^{-1} M^{-1} respectively. As for HO_2, the rate constants are 52.84 and 1.35 s^{-1} M^{-1} respectively. The atmospheric aqueous-phase lifetimes (τ) for GLY·1H_2O and GLY·2H_2O with O_3 were 6.09×10^{12} days and 8267 days, using O_3 concentration of 10^{-8} M.[56] The atmospheric aqueous-phase lifetimes (τ) for GLY·1H_2O and GLY·2H_2O towards HO_2 were 2.19×10^7 days and 8.57×10^8 days, using HO_2 concentration of 10^{-14} M.[56] Hence, the initial reactions of GLY with O_3 and HO_2 are much slower than GLY with OH radicals (761.45 days and 1714.68 days for GLY·1H_2O and GLY·2H_2O, respectively) and they are not that important in cloud/fog droplets.

3.3 Enhanced formate/formic acid formation in the presence of NO_2

In our analysis so far, although there are pathways that can form formic acid, oxalic acid is the most favorable product according to the reaction energetics (Fig. 2). However, our earlier work[26] reported that photooxidation of glyoxal mediated by particulate nitrate photolysis formed formic acid/formate, instead of oxalic acid and glyoxylic acid, as the major product. During particulate nitrate photolysis, in addition to OH radicals, reactive nitrogen species can also be formed during photolysis process. In addition, though NO_2 is one of abundant inorganic gas species in the atmosphere, its participation in the glyoxal oxidation has not been mechanistically examined. In this section, we examine how NO_2 modifies the glyoxal oxidation mechanisms and promotes the formation of formic acid/formate. Zhang *et al.*[26] reported that steady-state concentration of NO_2 can achieve to $\sim 10^{-8}$ M during glyoxal oxidation by particulate nitrate photolysis.[26] Furthermore, Mayorga *et al.*[57] found that the NO_2 pathway is the dominant pathway for the pyrrolyl radicals over peroxy radical chemistry in the aerosol phase at ambient-level NO_2 concentrations (90 ppb) even though concentration of O_2 is orders of magnitude higher than that of NO_2.[58,59] Saghafi *et al.*[60] and Augusto *et al.*[61] studied the hydrogen atom abstraction reaction of NO_2 in the gas phase, and hence we proposed the NO_2 abstraction reaction pathway for IM5.

In the presence of NO_2, IM5 formed from GLY·2H_2O (Fig. 2) can undergo further reactions in the aqueous phase. One pathway is the NO_2 addition to the carbon position and forms a nitro-product IM23 (Fig. 6). IM7 is formed after a HONO elimination reaction from IM23. IM7 can react with OH radical, followed by NO_2 addition and HONO elimination, to form oxalic acid P3. IM7 could also decompose into two formic acid (P4) molecules, but the energy barrier is 67.97 kcal mol^{-1}, too high for the reaction to occur. NO_2 can also abstract a H atom of IM5, resulting in the cleavage of C–C bond to form formic acid P4,

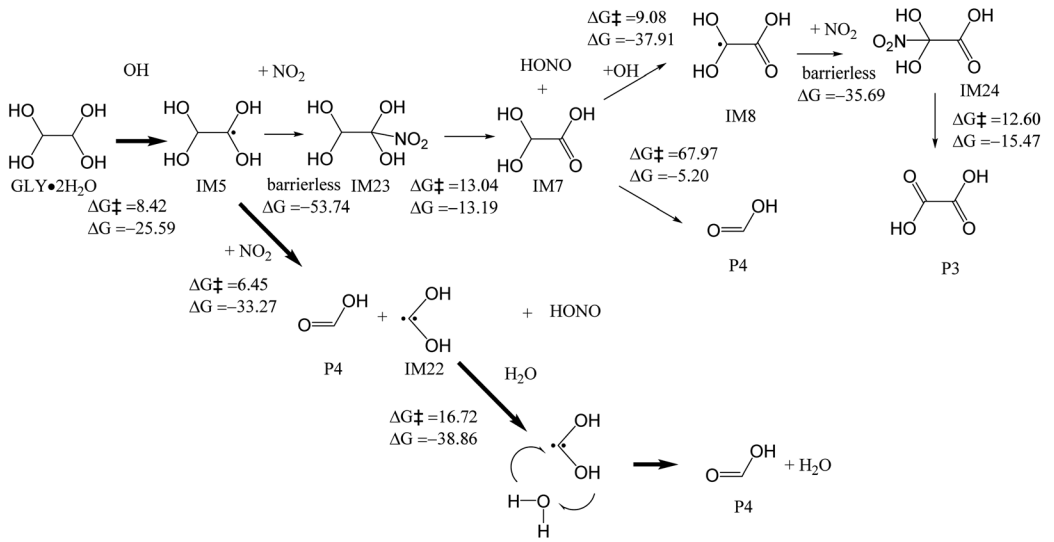

Fig. 6 Mechanisms for the reactions of GLY·2H_2O with NO_2 and OH in the aqueous phase, with the energy barrier ($\Delta G^{\ddagger}$) and reaction energy (ΔG) (kcal mol^{-1}), to yield formic acid.

HONO and IM22. This reaction is relatively fast because the energy barrier is only 6.45 kcal mol^{-1}. IM22 can also produce formic acid P4 through H transfer reaction involving water molecules, with the energy barrier of 16.72 kcal mol^{-1}. We also added the pathway of IM6 with NO_2 as a possibility (Fig. S5†). However, its energy barrier is 38.81 kcal mol^{-1}, higher than the pathway of IM5 with NO_2. Hence, it is not likely to occur.

In conclusion, formic acid can be formed *via* IM5 and IM22 (Fig. 6) in the presence of OH and NO_2. As depicted in Fig. 3a and b, it can also be formed in the presence of OH and O_2. The formation of glyoxylic acid and oxalic acid is also feasible in the presence of OH and O_2, as shown in Fig. 2 and 3c. On the basis of the rate constants of the related reactions (Table S1†), the reaction of IM5 with NO_2 to form formic acid is very fast, with the rate constants of 7.52×10^9 s^{-1} M^{-1}, which is in the same order of the reported overall rate constant of OH + GLY (4.5×10^{10} s^{-1} M^{-1}) in our earlier work.[26] The rate constants of reaction IM10 to IM11, IM15 to IM16, and IM17 to IM13 is 7.86×10^{-14} s^{-1} M^{-1}, 2.32×10^{-7} s^{-1} M^{-1}, and 3.51×10^{-25} s^{-1} M^{-1}, respectively; thus these pathways Fig. 3a–c are not feasible. The rate constants of the dominant reactions (in thick arrows) to form formic acid in Fig. 6 are between 10^5 and 10^7 s^{-1} M^{-1}. Hence, the formation of formic acid with the presence of NO_2 is the most favorable among all the pathways discussed. The mechanism above may explain why formic acid/formate is the predominant product in our earlier study of GLY oxidation under nitrate photolysis.[26]

3.4 Atmospheric implication

This work provides theoretical insights into the hydration, polymerization and oxidation mechanisms of GLY in the aqueous phase. Several previous studies[46,62,63] have reported that GLY exist in the form of hydrates and oligomers in SOA particulate phase, and GLY has been found to easily transfer from the gas phase to the aerosol phase at RH > 26%.[46] Our computational results showed that four or more water molecules are required to make the hydrolysis energetically favorable compared with the polymerization reaction. Hence hydrolysis is favored at high RH, whereas GLY polymerization is active at relatively low humidity levels. In addition, if other aldehyde molecules can be incorporated into glyoxal copolymers, as suggested by Kalberer *et al.*,[46,64] this process may partially explain the underprediction of the aerosol uptake of atmospheric aldehydes.

Recent studies found that glyoxal can be oxidized to produce formic acid, glyoxylic acid and oxalic acid in the aqueous phase under photochemical conditions.[20,25,65] The common dominant product in GLY oxidation were glyoxylic and oxalic acid, but we[26] reported earlier that formic acid was the main product in GLY oxidation under nitrate photolysis. This study showed that the formation of formic acid was more favorable in the presence of OH and NO_2. In the presence of OH and O_2, oxalic acid is the main product. The oxidation mechanisms of GLY towards HO_2, O_3 and H_2O_2 were also determined. Compared with OH radicals, the reactions of GLY with O_3 and HO_2 are quite slow and are of minor importance in the atmospheric liquid phase. Carlton *et al.*[25] expanded the mechanism of direct formic acid production from GLY through reactions with H_2O_2. Our theoretical results showed that although the H_2O_2 induced reactions can be competitive to that with OH radicals, the reactions with H_2O_2 are also not dominant pathways to form formic acid. NO_2 can be either from the gas-particle partitioning or generated from in-particle source, such as nitrate photolysis. Its presence might modify the oxidation processes initiated by OH radicals and change the product distribution. Since OH radicals and NO_2 both exist in the atmosphere, they should both be included in GLY oxidation mechanisms and have important implications for the role of GLY in SOA formation.

Conflicts of interest

There are no conflicts to declare.

Acknowledgements

This work was supported financially by the Hong Kong Research Grants Council (GRF 11302318, 11314222, 11304121), the National Natural Science Foundation of China (NSFC No. 21777087, 22206115, 22276109, 41875142, 42075100, and 42275104), the Shandong Provincial Natural Science Foundation Project ZR2022QB226, the CityU Strategic Research Grant 7005593, and the Hong Kong Scholars Program XJ2021029.

References

1 J. Yu, H. E. Jeffries and R. M. Le Lacheur, Identifying airborne carbonyl compounds in isoprene atmospheric photooxidation products by their PFBHA oximes using gas chromatography/ion trap mass spectrometry, *Environ. Sci. Technol.*, 1995, **29**, 1923–1932.
2 R. Volkamer, F. San Martini, L. T. Molina, D. Salcedo, J. L. Jimenez and M. J. Molina, A missing sink for gas-phase glyoxal in Mexico City: Formation of secondary organic aerosol, *Geophys. Res. Lett.*, 2007, **34**, L19807.
3 W. P. Carter and R. Atkinson, Development and evaluation of a detailed mechanism for the atmospheric reactions of isoprene and NOx, *Int. J. Chem. Kinet.*, 1996, **28**, 497–530.
4 H. Irie, K. Sudo, H. Akimoto, A. Richter, J. Burrows, T. Wagner, M. Wenig, S. Beirle, Y. Kondo and V. Sinyakov, Evaluation of long-term tropospheric NO2 data obtained by GOME over East Asia in 1996–2002, *Geophys. Res. Lett.*, 2005, **32**, L11810.
5 A. J. Kean, E. Grosjean, D. Grosjean and R. A. Harley, On-road measurement of carbonyls in California light-duty vehicle emissions, *Environ. Sci. Technol.*, 2001, **35**, 4198–4204.
6 E. Grosjean, P. G. Green and D. Grosjean, Liquid chromatography analysis of carbonyl (2, 4-dinitrophenyl) hydrazones with detection by diode array ultraviolet spectroscopy and by atmospheric pressure negative chemical ionization mass spectrometry, *Anal. Chem.*, 1999, **71**, 1851–1861.

7 B. Long, X.-f. Tan, D.-s. Ren and W.-j. Zhang, Theoretical study on the water-catalyzed reaction of glyoxal with OH radical, *J. Mol. Struct.: THEOCHEM*, 2010, **956**, 44–49.
8 B. Long, W.-j. Zhang, X.-f. Tan, Z.-w. Long, Y.-b. Wang and D.-s. Ren, Theoretical studies on the gas phase reaction mechanisms and kinetics of glyoxal with HO2 with water and without water, *Comput. Theor. Chem.*, 2011, **964**, 248–256.
9 Y. Li, Y. Ji, J. Zhao, Y. Wang, Q. Shi, J. Peng, Y. Wang, C. Wang, F. Zhang and Y. Wang, Unexpected oligomerization of small α-dicarbonyls for secondary organic aerosol and brown carbon formation, *Environ. Sci. Technol.*, 2021, **55**, 4430–4439.
10 Y. Lim, Y. Tan, M. Perri, S. Seitzinger and B. Turpin, Aqueous chemistry and its role in secondary organic aerosol (SOA) formation, *Atmos. Chem. Phys.*, 2010, **10**, 10521–10539.
11 B. Ervens and R. Volkamer, Glyoxal processing by aerosol multiphase chemistry: towards a kinetic modeling framework of secondary organic aerosol formation in aqueous particles, *Atmos. Chem. Phys.*, 2010, **10**, 8219–8244.
12 J. H. Kroll, N. L. Ng, S. M. Murphy, V. Varutbangkul, R. C. Flagan and J. H. Seinfeld, Chamber studies of secondary organic aerosol growth by reactive uptake of simple carbonyl compounds, *J. Geophys. Res.: Atmos.*, 2005, **110**, D23207.
13 H. S. Ip, X. H. Huang and J. Z. Yu, Effective Henry's law constants of glyoxal, glyoxylic acid, and glycolic acid, *Geophys. Res. Lett.*, 2009, **36**, L01802.
14 F. Zhang, X. Yu, X. Sui, J. Chen, Z. Zhu and X.-Y. Yu, Evolution of aqsoa from the air–liquid interfacial photochemistry of glyoxal and hydroxyl radicals, *Environ. Sci. Technol.*, 2019, **53**, 10236–10245.
15 V. F. McNeill, Aqueous organic chemistry in the atmosphere: sources and chemical processing of organic aerosols, *Environ. Sci. Technol.*, 2015, **49**(3), 1237–1244.
16 J. Lockhart, M. Blitz, D. Heard, P. Seakins and R. Shannon, Kinetic study of the OH+ glyoxal reaction: experimental evidence and quantification of direct OH recycling, *J. Phys. Chem. A*, 2013, **117**, 11027–11037.
17 O. Setokuchi, Trajectory calculations of OH radical-and Cl atom-initiated reaction of glyoxal: atmospheric chemistry of the HC (O) CO radical, *Phys. Chem. Chem. Phys.*, 2011, **13**, 6296–6304.
18 H. Niki, P. Maker, C. Savage and L. Breitenbach, An FTIR study of the Cl-atom-initiated reaction of glyoxal, *Int. J. Chem. Kinet.*, 1985, **17**, 547–558.
19 T. Schaefer, D. Van Pinxteren and H. Herrmann, Multiphase chemistry of glyoxal: Revised kinetics of the alkyl radical reaction with molecular oxygen and the reaction of glyoxal with OH, NO3, and SO4–in aqueous solution, *Environ. Sci. Technol.*, 2015, **49**, 343–350.
20 Y. Tan, M. J. Perri, S. P. Seitzinger and B. J. Turpin, Effects of precursor concentration and acidic sulfate in aqueous glyoxal– OH radical oxidation and implications for secondary organic aerosol, *Environ. Sci. Technol.*, 2009, **43**, 8105–8112.
21 A. K. Lee, R. Zhao, S. Gao and J. Abbatt, Aqueous-phase OH oxidation of glyoxal: application of a novel analytical approach employing aerosol mass spectrometry and complementary off-line techniques, *J. Phys. Chem. A*, 2011, **115**, 10517–10526.
22 A. Laskin, J. Laskin and S. A. Nizkorodov, Chemistry of atmospheric brown carbon, *Chem. Rev.*, 2015, **115**, 4335–4382.
23 D. L. Ortiz-Montalvo, S. A. Häkkinen, A. N. Schwier, Y. B. Lim, V. F. McNeill and B. J. Turpin, Ammonium addition (and aerosol pH) has a dramatic impact on the volatility and yield of glyoxal secondary organic aerosol, *Environ. Sci. Technol.*, 2014, **48**, 255–262.
24 N. Sedehi, H. Takano, V. A. Blasic, K. A. Sullivan and D. O. De Haan, Temperature-and pH-dependent aqueous-phase kinetics of the reactions of glyoxal and methylglyoxal with atmospheric amines and ammonium sulfate, *Atmos. Environ.*, 2013, **77**, 656–663.
25 A. G. Carlton, B. J. Turpin, K. E. Altieri, S. Seitzinger, A. Reff, H.-J. Lim and B. Ervens, Atmospheric oxalic acid and SOA production from glyoxal: Results of aqueous photooxidation experiments, *Atmos. Environ.*, 2007, **41**, 7588–7602.
26 R. Zhang, M. Gen, T.-M. Fu and C. K. Chan, Production of formate via oxidation of glyoxal promoted by particulate nitrate photolysis, *Environ. Sci. Technol.*, 2021, **55**, 5711–5720.
27 S. Goldstein and J. Rabani, Mechanism of nitrite formation by nitrate photolysis in aqueous solutions: the role of peroxynitrite, nitrogen dioxide, and hydroxyl radical, *J. Am. Chem. Soc.*, 2007, **129**, 10597–10601.
28 S. Goldstein, J. Lind and G. Merényi, Chemistry of peroxynitrites as compared to peroxynitrates, *Chem. Rev.*, 2005, **105**, 2457–2470.
29 M. Frisch, G. Trucks, H. Schlegel, G. Scuseria, M. Robb, J. Cheeseman, G. Scalmani, V. Barone, G. Petersson and H. Nakatsuji, *Gaussian 16 Rev. C. 01*, 2016.
30 Y. Zhao and D. G. Truhlar, The M06 suite of density functionals for main group thermochemistry, thermochemical kinetics, noncovalent interactions, excited states, and transition elements: two new functionals and systematic testing of four M06-class functionals and 12 other functionals, *Theor. Chem. Acc.*, 2008, **120**, 215–241.
31 B. Long, X.-F. Tan, C.-R. Chang, W.-X. Zhao, Z.-W. Long, D.-S. Ren and W.-J. Zhang, Theoretical studies on gas-phase reactions of sulfuric acid catalyzed hydrolysis of formaldehyde and formaldehyde with sulfuric acid and H2SO4⋯ H2O complex, *J. Phys. Chem. A*, 2013, **117**, 5106–5116.
32 F.-Y. Liu, X.-F. Tan, Z.-W. Long, B. Long and W.-J. Zhang, New insights in atmospheric acid-catalyzed gas phase hydrolysis of formaldehyde: a theoretical study, *RSC Adv.*, 2015, **5**, 32941–32949.
33 B. Wei, J. Sun, Q. Mei, Z. An, X. Wang and M. He, Theoretical study on gas-phase reactions of nitrate radicals with methoxyphenols: Mechanism, kinetic and toxicity assessment, *Environ. Pollut.*, 2018, **243**, 1772–1780.

34 B. Wei, J. Sun, Q. Mei, Z. An, H. Cao, D. Han, J. Xie, J. Zhan, Q. Zhang and W. Wang, Reactivity of aromatic contaminants towards nitrate radical in tropospheric gas and aqueous phase, *J. Hazard. Mater.*, 2021, **401**, 123396.

35 A. V. Marenich, C. J. Cramer and D. G. Truhlar, Universal solvation model based on solute electron density and on a continuum model of the solvent defined by the bulk dielectric constant and atomic surface tensions, *J. Phys. Chem. B*, 2009, **113**, 6378–6396.

36 S. Canneaux, F. Bohr and E. Henon, KiSThelP: a program to predict thermodynamic properties and rate constants from quantum chemistry results, *J. Comput. Chem.*, 2014, **35**, 82–93.

37 C. Zhu, S. Kais, X. C. Zeng, J. S. Francisco and I. Gladich, Interfaces select specific stereochemical conformations: the isomerization of glyoxal at the liquid water interface, *J. Am. Chem. Soc.*, 2017, **139**, 27–30.

38 E. Avzianova and S. D. Brooks, Raman spectroscopy of glyoxal oligomers in aqueous solutions, *Spectrochim. Acta, Part A*, 2013, **101**, 40–48.

39 M. K. Hazra, J. S. Francisco and A. Sinha, Hydrolysis of glyoxal in water-restricted environments: formation of organic aerosol precursors through formic acid catalysis, *J. Phys. Chem. A*, 2014, **118**, 4095–4105.

40 E. B. Whipple, Structure of glyoxal in water, *J. Am. Chem. Soc.*, 1970, **92**, 7183–7186.

41 F. Chastrette, C. Bracoud, M. Chastrette, G. Mattioda and Y. Christidis, Etude de la composition de solutions aqueuses de glyoxal en RMN-^{13}C, *Bull. Soc. Chim. Fr.*, 1983, (1−2), II33–II40.

42 F. Chastrette, C. Bracoud, M. Chastrette, G. Mattioda and Y. Christidis, Etude de la composition de solutions aqueuses d'acide glyoxylique en RMN de 13C, *Bull. Soc. Chim. Fr.*, 1985, 66–74.

43 H. A. Rypkema, A. Sinha and J. S. Francisco, Carboxylic acid catalyzed hydration of acetaldehyde, *J. Phys. Chem. A*, 2015, **119**, 4581–4588.

44 R. Volkamer, P. Ziemann and M. Molina, Secondary Organic Aerosol Formation from Acetylene (C2H2): seed effect on SOA yields due to organic photochemistry in the aerosol aqueous phase, *Atmos. Chem. Phys.*, 2009, **9**, 1907–1928.

45 G. Michailoudi, J. J. Lin, H. Yuzawa, M. Nagasaka, M. Huttula, N. Kosugi, T. Kurtén, M. Patanen and N. L. Prisle, Aqueous-phase behavior of glyoxal and methylglyoxal observed with carbon and oxygen K-edge X-ray absorption spectroscopy, *Atmos. Chem. Phys.*, 2021, **21**, 2881–2894.

46 W. P. Hastings, C. A. Koehler, E. L. Bailey and D. O. De Haan, Secondary organic aerosol formation by glyoxal hydration and oligomer formation: Humidity effects and equilibrium shifts during analysis, *Environ. Sci. Technol.*, 2005, **39**, 8728–8735.

47 Y. Lim, Y. Tan and B. Turpin, Chemical insights, explicit chemistry, and yields of secondary organic aerosol from OH radical oxidation of methylglyoxal and glyoxal in the aqueous phase, *Atmos. Chem. Phys.*, 2013, **13**, 8651–8667.

48 E. Hellpointner and S. Gäb, Detection of methyl, hydroxymethyl and hydroxyethyl hydroperoxides in air and precipitation, *Nature*, 1989, **337**, 631–634.

49 Y. Tan, Y. Lim, K. Altieri, S. Seitzinger and B. Turpin, Mechanisms leading to oligomers and SOA through aqueous photooxidation: insights from OH radical oxidation of acetic acid and methylglyoxal, *Atmos. Chem. Phys.*, 2012, **12**, 801–813.

50 A. K. Lee, P. Herckes, W. Leaitch, A. Macdonald and J. Abbatt, Aqueous OH oxidation of ambient organic aerosol and cloud water organics: Formation of highly oxidized products, *Geophys. Res. Lett.*, 2011, **38**, L11805.

51 Z. Sun, W. Eli, T. Xu and Y. Zhang, Oxidation of glyoxal with hydroperoxide compounds prepared from maleic acid by ozonation to produce glyoxylic acid, *Ind. Eng. Chem. Res.*, 2006, **45**, 1849–1852.

52 M. Mucha and Z. Mielke, Photochemistry of the glyoxal–hydrogen peroxide complexes in solid argon: Formation of 2-hydroxy-2-hydroperoxyethanal, *Chem. Phys. Lett.*, 2009, **482**, 87–92.

53 S. Myriokefalitakis, K. Tsigaridis, N. Mihalopoulos, J. Sciare, A. Nenes, K. Kawamura, A. Segers and M. Kanakidou, In-cloud oxalate formation in the global troposphere: a 3-D modeling study, *Atmos. Chem. Phys.*, 2011, **11**, 5761–5782.

54 J. M. Anglada and V. M. Domingo, Mechanism for the gas-phase reaction between formaldehyde and hydroperoxyl radical. A theoretical study, *J. Phys. Chem. A*, 2005, **109**, 10786–10794.

55 G. da Silva, Kinetics and Mechanism of the Glyoxal+ HO2 Reaction: Conversion of HO2 to OH by Carbonyls, *J. Phys. Chem. A*, 2011, **115**, 291–297.

56 Y. M. Gershenzon, S. Zvenigorodskii and V. Rozenshtein, The chemistry of OH and HO2 radicals in the earth's atmosphere, *Russ. Chem. Rev.*, 1990, **59**, 928.

57 R. Mayorga, K. Chen, N. Raeofy, M. Woods, M. Lum, Z. Zhao, W. Zhang, R. Bahreini, Y. H. Lin and H. Zhang, Chemical Structure Regulates the Formation of Secondary Organic Aerosol and Brown Carbon in Nitrate Radical Oxidation of Pyrroles and Methylpyrroles, *Environ. Sci. Technol.*, 2022, **56**(12), 7761–7770.

58 J. Platz, O. Nielsen, T. Wallington, J. Ball, M. Hurley, A. Straccia, W. Schneider and J. Sehested, Atmospheric chemistry of the phenoxy radical, C6H5O (˙): UV spectrum and kinetics of its reaction with NO, NO2, and O2, *J. Phys. Chem. A*, 1998, **102**, 7964–7974.

59 Z. Finewax, J. A. de Gouw and P. J. Ziemann, Identification and quantification of 4-nitrocatechol formed from OH and NO3 radical-initiated reactions of catechol in air in the presence of NOx: implications for secondary organic aerosol formation from biomass burning, *Environ. Sci. Technol.*, 2018, **52**, 1981–1989.

60 H. Saghafi and M. Vahedpour, Atmospheric reactions of glyoxal with NO2 and NH2 radicals: hydrogen abstraction mechanism and natural bond orbital analysis, *Prog. React. Kinet. Mech.*, 2019, **44**, 187–209.

61 O. Augusto, M. G. Bonini, A. M. Amanso, E. Linares, C. C. Santos and S. l. L. De Menezes, Nitrogen dioxide and

carbonate radical anion: two emerging radicals in biology, *Free Radicals Biol. Med.*, 2002, **32**, 841–859.

62 M. Hoffmann, M. Igawa and J. Munger, Analysis of Aldehydes in Cloud- and Fogwater Samples by HPLC with a Postcolumn Reaction Detector, *Environ. Sci. Technol.*, 1989, **23**(5), 556–561.

63 J. Liggio, S.-M. Li and R. McLaren, Heterogeneous reactions of glyoxal on particulate matter: Identification of acetals and sulfate esters, *Environ. Sci. Technol.*, 2005, **39**, 1532–1541.

64 M. Kalberer, D. Paulsen, M. Sax, M. Steinbacher, J. Dommen, A. S. Prévôt, R. Fisseha, E. Weingartner, V. Frankevich and R. Zenobi, Identification of polymers as major components of atmospheric organic aerosols, *Science*, 2004, **303**, 1659–1662.

65 X. Sui, Y. Zhou, F. Zhang, J. Chen, Z. Zhu and X.-Y. Yu, Deciphering the aqueous chemistry of glyoxal oxidation with hydrogen peroxide using molecular imaging, *Phys. Chem. Chem. Phys.*, 2017, **19**, 20357–20366.